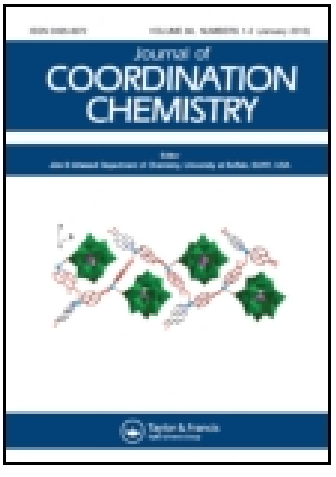

Journal of Coordination Chemistry
Publication details, including instructions for authors and subscription information:
http://www.tandfonline.com/loi/gcoo20

Synthesis, characterization, and biocide activity of new dithiocarbamate-based complexes of In(III), Ga(III), and Bi(III) - Part III

I.P. Ferreira[a], G.M. de Lima[a], E.B. Paniago[a], J.A. Takahashi[a] & C.B. Pinheiro[b]

[a] Departamento de Química, Universidade Federal de Minas Gerais, Belo Horizonte, Brazil

[b] Laboratório de Cristalografia, Departamento de Física, Universidade Federal de Minas Gerais, Belo Horizonte, Brazil

Accepted author version posted online: 25 Mar 2014.Published online: 15 Apr 2014.

To cite this article: I.P. Ferreira, G.M. de Lima, E.B. Paniago, J.A. Takahashi & C.B. Pinheiro (2014) Synthesis, characterization, and biocide activity of new dithiocarbamate-based complexes of In(III), Ga(III), and Bi(III) - Part III, Journal of Coordination Chemistry, 67:6, 1097-1109, DOI: 10.1080/00958972.2014.908188

To link to this article: http://dx.doi.org/10.1080/00958972.2014.908188

Journal of Coordination Chemistry, 2014
Vol. 67, No. 6, 1097–1109, http://dx.doi.org/10.1080/00958972.2014.908188

Synthesis, characterization, and biocide activity of new dithiocarbamate-based complexes of In(III), Ga(III), and Bi(III) – Part III

I.P. FERREIRA†, G.M. DE LIMA*†, E.B. PANIAGO†, J.A. TAKAHASHI† and C.B. PINHEIRO‡

†Departamento de Química, Universidade Federal de Minas Gerais, Belo Horizonte, Brazil
‡Laboratório de Cristalografia, Departamento de Física, Universidade Federal de Minas Gerais, Belo Horizonte, Brazil

(*Received 27 November 2013; accepted 26 February 2014*)

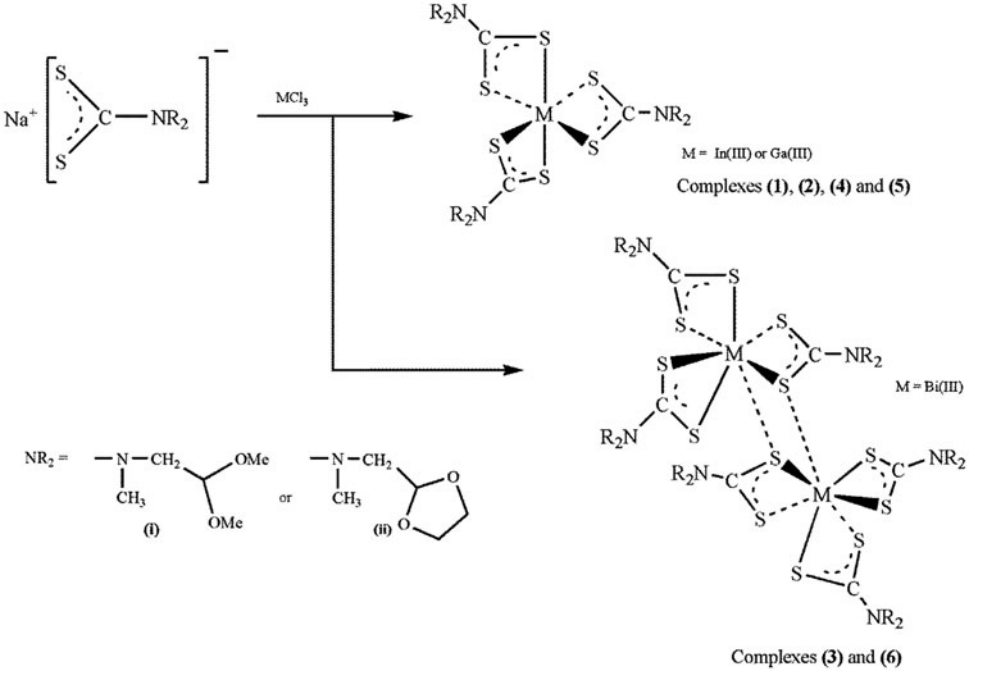

In this work, we describe the syntheses, characterization, and antifungal activity of [In{$S_2CNR(R^1)$}$_3$] (**1**), [Ga{$S_2CNR(R^1)$}$_3$] (**2**), [Bi{$S_2CNR(R^1)$}$_3$] (**3**), [In{$S_2CNR(R^2)$}$_3$] (**4**), [Ga{$S_2CNR(R^2)$}$_3$] (**5**), and [Bi{$S_2CNR(R^2)$}$_3$] (**6**) {R = Me; $R^1 = CH_2CH(OMe)_2$; and R^2 = 2-methyl-1,3-dioxolane}. All complexes

*Corresponding author. Email: gmlima@ufmg.br

have been characterized using infrared and ^{1}H and ^{13}C spectroscopy, and the structures of **1**, **3**, **4**, and **6** have been authenticated by X-ray diffraction. The In(III)–dithiocarbamate bonding scheme depicts a distorted octahedral with asymmetric In(III)–S bonds and S–In–S angles. A pentagonal bipyramid is observed for the corresponding Bi(III) complexes with intermolecular Bi–S associations through the lone pair of electrons. The antifungal activities of **1–6** have been screened against *Aspergillus niger*, *Aspergillus parasiticus*, and *Penicillium citrinum*, and the results have been compared with those of nystatin and miconazole nitrate, as control drugs.

Keywords: Dithiocarbamate; Antifungal activity; Main group cations

1. Introduction

Dithiocarbamates (DTC) and dithiophosphates are useful ligands in coordination chemistry with a variety of molecular and supramolecular structures documented [1, 2]. In addition, they find applications in a wide range of fields. Apart from their ability to stabilize metal cations in diverse oxidation states, their pharmaceutical properties are noteworthy [3]. They are used to remove excess copper due to Wilson's disease [4], they are also able to reduce the nephrotoxicity of platinum-based drugs used in chemotherapy [5], and in addition, they are effective in the treatment of alcoholism [6] or in other clinical applications [7]. In addition, they find applications in rubber vulcanization [8], preparation of pesticides [9], and as precursors for production of metal sulfide nanoparticles [10].

Bismuth has been employed for many centuries in human disease treatment. Today, bismuth subcitrate or subgallate are effective in the eradication of *Helicobacter pylori*, a bacterium associated with gastro-duodenal pathogenesis [11]. Moreover, anticancer and antitumor activity [12] and other antimicrobial properties have been observed for some Bi(III) DTC [13].

The coordination chemistry of Ga(III) has attracted attention in the last few years for radioisotopic applications of its complexes and potential chemotherapeutic properties [14]. Some gallium complexes, tris(8-quinolinolato)gallium(III) [15] and tris(3-hydroxy-2-methyl-4H-pyran-4-onato)gallium(III) [16], have been selected for clinical studies. Articles describing the antimicrobial activity of Ga(III)-thiosemicarbazones have been published recently [17, 18].

Indium-based potential radiopharmaceuticals have been widely investigated *in vitro* and *in vivo* by NMR spectroscopy. Despite interest in In(III) macrocyclic complexes for imaging or radioimmunotherapy applications [19], the literature is scarce concerning antimicrobial studies of In(III)-containing complexes.

Most DTC-containing complexes reported have simple R^1 and R^2 groups such as methyl, ethyl, phenyl, etc. We have been interested in attaching less simple DTC ligands to metal cations, for example $R^1 = -CH_2CH(OMe)_2$ and $R^2 = 2$-methyl-1,3-dioxolane, in order to evaluate their biocide responses as a consequence of the new bonding, or the chemical and structural properties. Following our interest on this [20–26], herein, we describe the synthesis, characterization, and crystallographic authentication of $[In\{S_2CNR(R^1)\}_3]$ (**1**), $[Ga\{S_2CNR(R^1)\}_3]$ (**2**), $[Bi\{S_2CNR(R^1)\}_3]$ (**3**), $[In\{S_2CNR(R^2)\}_3]$ (**4**), $[Ga\{S_2CNR(R^2)\}_3]$ (**5**) and $[Bi\{S_2CNR(R^2)\}_3]$ (**6**) {$R = Me$; $R^1 = CH_2CH(OMe)_2$, and $R^2 = 2$-methyl-1,3-dioxolane}. In addition, we have screened the biological activity of **1–6** against *Aspergillus niger*, *Aspergillus parasiticus*, and *Penicillium citrinum*.

2. Experimental setup

2.1. *Materials and instruments*

Starting materials were purchased from Aldrich, Merck, or Synth and used as received. NMR spectra were recorded at 400 MHz using a Bruker DPX-400 spectrometer equipped with an 89 mm wide-bore magnet. ^{1}H and ^{13}C shifts are reported relative to $SiMe_4$. Infrared spectra were recorded with samples pressed as KBr pellets on a Perkin-Elmer GX FT-IR spectrometer from 4000 to 200 cm^{-1}. Carbon, hydrogen, and nitrogen analyses were performed on a Perkin-Elmer PE-2400 CHN-analysis using tin sample tubes. Intensity data for single crystals of **1**, **3**, **4**, and **6** were collected at 290 K on an Oxford-Diffraction GEMINI diffractometer (LabCri) using Cu Kα radiation ($\lambda = 1.54184$ Å), based at the Physics Department, UFMG, Brazil. Data integration, scaling of the reflections for all compounds, and analytical and semi-empirical absorption corrections were performed with the *Crysalis* suite [27]. Final unit cell parameters were based on the fitting of all reflection positions. *XPREP* [27] was used in the space group identification. The structures of the compounds were solved by direct methods using the *SHELXS* [28] program. The positions of all atoms could be unambiguously assigned from consecutive difference Fourier maps. Refinements were performed using *SHELXL* [28] based on F^2 through full-matrix least square. All non-H atoms were refined anisotropically. The hydrogens in the compounds were added in idealized positions and further refined according to the riding model [29]. The ORTEP-3 program for windows [30] was used in the preparation of figures 1–4, sketched employing the Mercury program [31].

2.2. *Syntheses*

The DTC $Na[S_2CNR(R^1)]$ **(i)** and $Na[S_2CNR(R^2)]$ **(ii)** R = Me; $R^1 = CH_2CH(OMe)_2$, R^2 = 2-methyl-1,3-dioxolane have been previously prepared [32].

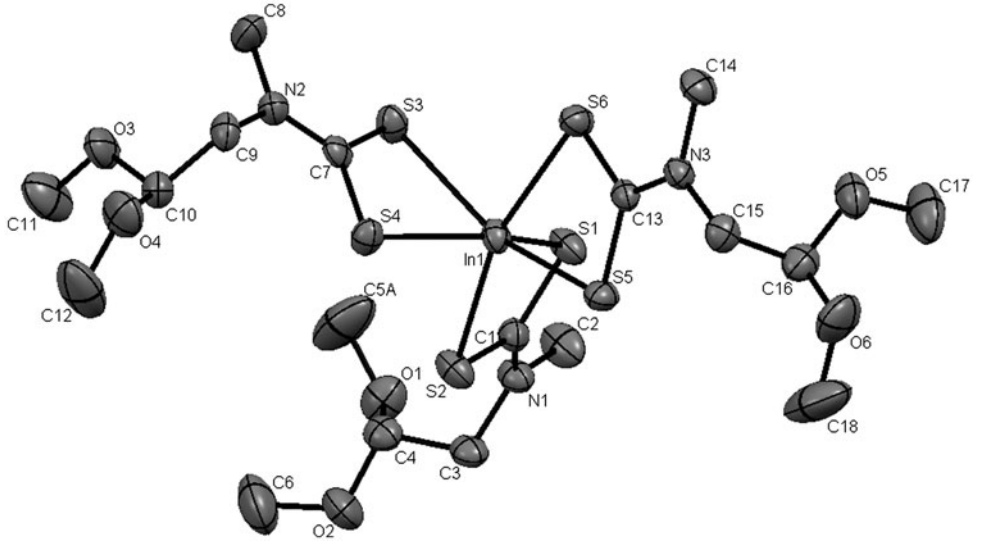

Figure 1. The molecular structure of **1**.

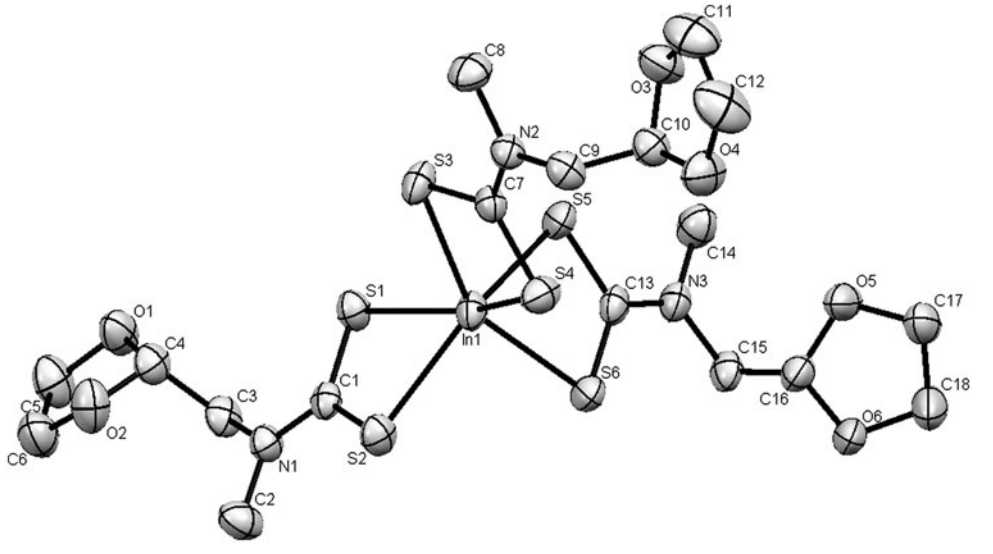

Figure 2. The molecular structure of **4**.

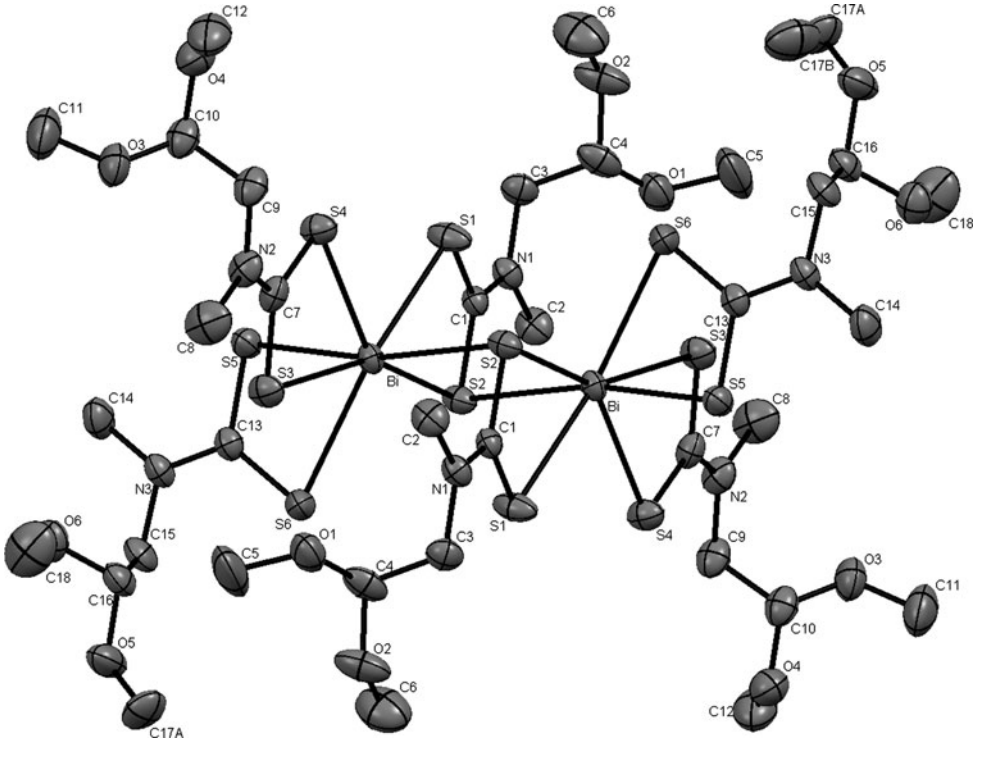

Figure 3. The molecular structure of **3**.

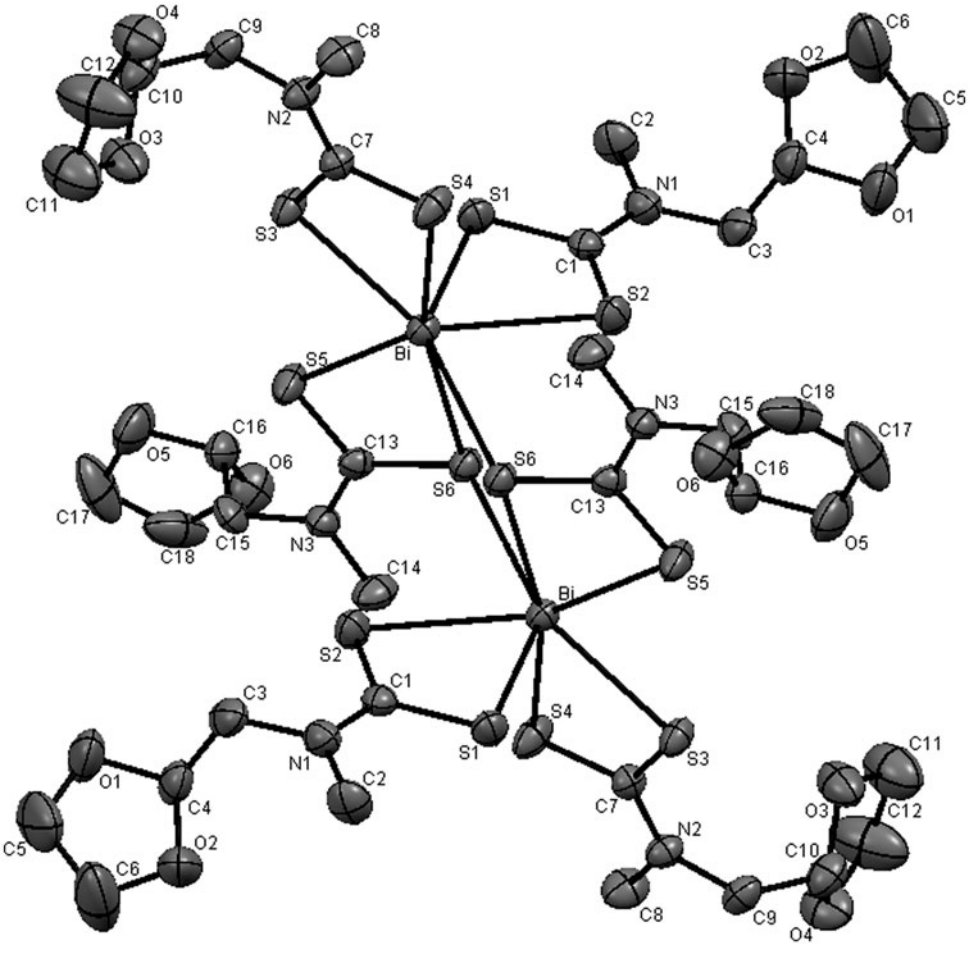

Figure 4. The molecular structure of **6**.

2.2.1. [In{$S_2CNR(R^1)$}$_3$] (1). {R = Me and $R^1 = CH_2CH(OMe)_2$}: To an aqueous suspension of [In{CH_3COO}$_3$] (1.0 g, 3.4 mM), an aqueous solution of **(i)** (2.2 g, 10.3 mM) was slowly added by stirring at room temperature. A white precipitate was immediately formed and the mixture stirred for 1 h. The product was filtered, washed with an excess of distilled water, dissolved in ethyl alcohol, and filtered. The filtrate was dried in vacuum and recrystallized from a mixture of acetone and ethanol (2 : 1) affording X-ray quality crystals of **1**. Yield 91%. M.p. 139.2–140.7 °C (dec). IR (cm^{-1}, KBr): 1496 (ν_{N-CS}); 982 {$\nu_{asym\ (C-S)}$}; 614 {$\nu_{sym\ (C-S)}$}. ^{1}H NMR (δ, $CDCl_3$): 4.80 (s) (C*H*); 3.89 ($^2J_{HH}$ = 4.0 Hz) (d) (NCH_2); 3.48 (s) (NCH_3) and 3.45 (s) (OCH_3). ^{13}C NMR (δ, $CDCl_3$): 202.3 (*C*S_2); 102.3 (*C*H); 60.4 (N*C*H_2); 55.3 (O*C*H_3); 46.3 (N*C*H_3). Analysis for $C_{18}H_{36}N_3O_6S_6In$: found (Calcd) C 30.15 (30.99); H 5.09 (5.20); N 5.94 (6.02).

Complexes **2–6** were prepared similar to **1**.

2.2.2. [Ga{$S_2CNR(R^1)$}$_3$] (2). {R = Me and $R^1 = CH_2CH(OMe)_2$}: Synthesized using [Ga{NO_3}$_3$] (1.0 g, 3.9 mM) and **(i)** (2.5 g, 11.7 mM). Yield 81%. M.p. 82.1–90.0 °C (dec). IR

(cm^{-1}, KBr): 1498 ($\nu_{N–CS}$); 994 {$\nu_{asym\ (C–S)}$}; 616 {$\nu_{sym\ (C–S)}$}. ^{1}H NMR (δ, $CDCl_3$): 4.76 (s)(C*H*); 3.84 ($^2J_{HH}$ = 3.9 Hz) (d) (NCH_2); 3.46 (s) (NCH_3) and 3.44 (s) (OCH_3). ^{13}C NMR (δ, $CDCl_3$): 208.5 (*C*S_2); 102.3 (*C*H); 55.3 (O*C*H_3); 53.1 (N*C*H_2); 38.6 (N*C*H_3). Analysis for $C_{18}H_{36}N_3O_6S_6$Ga: found (Calcd) C 33.65 (33.13); H 5.18 (5.56); N 6.97 (6.44).

2.2.3. [Bi{$C_6H_{12}NO_2S_2$}$_3$] (3). {R = Me and R^1 = $CH_2CH(OMe)_2$}: It was obtained by employing [Bi{NO_3}$_3$·5H_2O] (1.0 g, 2.1 mM) and **(i)** (1.3 g, 6.2 mM). The yellow solid obtained was isolated and re-crystallized from dichloromethane–ethanol (4 : 1). Yellow X-ray quality crystals of **3** were obtained by evaporation of the solvent at room temperature. Yield 94%. M.p. 125.4–126.7 °C (dec). IR (cm^{-1}, KBr): 1489 ($\nu_{N–CS}$); 977 {$\nu_{asym(C–S)}$}; 657 {$\nu_{sym(C–S)}$}. ^{1}H NMR (δ, $CDCl_3$): 4.81 (s) (C*H*); 3.90 ($^2J_{HH}$ = 4.0 Hz) (d) (NCH_2); 3.47 (s) (NCH_3) and 3.44 (s) (OCH_3). ^{13}C NMR (δ, $CDCl_3$): 203.5 (*C*S_2); 102.5 (*C*H); 58.3 (N*C*H_2); 55.3 (O*C*H_3); 44.3 (N*C*H_3). Analysis for $C_{18}H_{36}N_3O_6S_6Bi$: found (Calcd) C 27.29 (27.31); H 4.45 (4.58); N 5.28 (5.31).

2.2.4. [In{$S_2CNR(R^2)$}$_3$] (4). {R = Me and R^2 = 2-methyl-1,3-dioxolane}: Prepared using [In{CH_3COO}$_3$] (1.0 g, 3.4 mM) and **(ii)** (2.2 g, 10.3 mM). X-ray quality crystals of **4** were obtained from a mixture of acetone and ethanol (2 : 1). Yield 94%. M.p. 165.2–166.9 °C (dec). IR (cm^{-1}, KBr): 1501 ($\nu_{N–CS}$); 988 {$\nu_{asym\ (C–S)}$}; 604 {$\nu_{sym\ (C–S)}$}. ^{1}H NMR (δ, CD_2Cl_2): 5.45 ($^2J_{HH}$ = 6.0 Hz) (t) (OC*H*O); 3.93 (m) (OCH_2); 4.03 ($^2J_{HH}$ = 5.5 Hz) (d) (NCH_2) and 3.47 (s) (NCH_3). ^{13}C NMR (δ, CD_2Cl_2): 204.4 (*C*S_2); 101.1 (O*C*HO); 65.4 (O*C*H_2); 60.9 (N*C*H_2); 46.1 (N*C*H_3). Analysis for $C_{18}H_{30}N_3O_6S_6In$: found (Calcd) C 31.28 (31.27); H 4.35 (4.37); N 6.14 (6.08).

2.2.5. [Ga{$S_2CNR(R^1)$}$_3$] (5). {R = Me and R^2 = 2-methyl-1,3-dioxolane}: Obtained using [Ga{NO_3}$_3$] (1.0 g, 3.9 mM) and **(ii)** (2.5 g, 11.7 mM). Yield 76%. M.p. 94.4–95.9 °C (dec). IR (cm^{-1}, KBr): 1498 ($\nu_{N–CS}$); 991 {$\nu_{asym\ (C–S)}$}; 600 {$\nu_{sym\ (C–S)}$}. ^{1}H NMR (δ, $CDCl_3$): 5.13 ($^2J_{HH}$ = 8.0 Hz) (t) (OC*H*O); 3.49 (m) (OCH_2); 4.23 ($^2J_{HH}$ = 5.3 Hz) (d) (NCH_2) and 3.36 (s) (NCH_3). ^{13}C NMR (δ, $CDCl_3$): 202.2 (*C*S_2); 101.1 (O*C*HO); 64.4 (O*C*H_2); 58.8 (N*C*H_2); 44.3 (N*C*H_3). Analysis for $C_{18}H_{30}N_3O_6S_6$Ga: found (Calcd) C 33.23 (33.44); H 4.59 (4.67); N 6.48 (6.50).

2.2.6. [Bi{$S_2CNR(R^1)$}$_3$] (6). {R = Me and R^2 = 2-methyl-1,3-dioxolane}: It was prepared utilizing [Bi{NO_3}$_3$·5H_2O] (1.0 g, 2.1mM) and **(ii)** (1.3 g, 6.2 mM). The solid formed was re-crystallized from a mixture of dichloromethane and ethanol (2 : 1), yielding yellow crystals of **6** suitable for X-ray crystallography. Yield 95%. M.p. 150.4–151.4 °C (dec). IR (cm^{-1}, KBr): 1490 ($\nu_{N–CS}$); 977 {$\nu_{asym(C–S)}$}; 606 {$\nu_{sym(C–S)}$}. ^{1}H NMR (δ, $CDCl_3$): 5.24 ($^2J_{HH}$ = 4.1 Hz) (d) (OC*H*O); 3.85 (m) (OCH_2); 3.97 ($^2J_{HH}$ = 3.3 Hz) (d) NCH_2) and 3.44 (s) (NCH_3). ^{13}C NMR (δ, $CDCl_3$): 203.9 (*C*S_2); 101.1 (O*C*HO); 64.8 (O*C*H_2); 58.2 (N*C*H_2); 43.6 (N*C*H_3). Analysis for $C_{18}H_{30}N_3O_6S_6Bi$: found (Calcd) C 27.61 (27.52); H 3.31 (3.85); N 5.41 (5.35).

2.3. *Biological tests*

A. niger (NRRL 3), *A. parasiticus* (ATCC 15517), and *P. citrinum* (ATCC 756) were obtained from the ARS Culture Collection (NRRL, USA), American Type Culture

Collection (ATCC, USA) and Biotechnology and Bioassays Laboratory (LABB, MG, Brazil). They were kept in potato dextrose agar under refrigeration at 7 °C. The tests were performed in Broth Heart Infusion (BHI) medium. Fungal spores were counted in a Neubauer chamber. Dilutions were carried out to achieve the required final concentration of spores of 5.0×10^3 spores mL^{-1}. The dithiocarbamate complexes, nystatin, and miconazole nitrate were prepared as 12.5 mg mL^{-1} stock solutions in DMSO. Subsequently, the stock solutions were diluted in BHI obtaining 500 μg mL^{-1} solutions. Further dilutions of each antifungal agent were performed in BHI medium. The wells of microdilution plates were filled with 100 μL of solutions with decreasing concentrations of the antimicrobial agent in culture medium. Then, 100 μL of the solution containing the standardized inocula was added and the microplates were incubated at 37 °C for 24 and 48 h for antifungal tests. Controls were performed for evaluating the growth of micro-organisms in culture medium without any compound (positive control) and with the compounds to assure the sterility of the culture medium. Tests with the reference compounds, nystatin, and miconazole nitrate were also carried out (negative controls). The experiments were carried out in triplicate and the absorbances were determined on an ELISA tray reader (Thermoplate, Brazil) at 492 nm. MICs were calculated based on the quantity of the micro-organism present after the experiments, i.e. the lowest concentration of compounds that resulted in a 50% (MIC_{50}) or 90% (MIC_{90}) reduction of growth compared with the control growth in the culture medium free of the test compound.

3. Results and discussion

3.1. *Synthesis*

Complexes **1–6** (scheme 1) have been isolated as air-stable crystalline solids in yields varying from 45 to 95%. Except **3** and **6** that are yellow, the other complexes were obtained as white materials. The purity of **1–6** has been attested in terms of satisfactory melting points and C, H, and N analyses.

3.2. *Spectroscopic characterization*

The infrared spectra of the metal dithiocarbamate complexes are an important tool in the analysis of the coordination mode of DTC, as well as their M–S bonds [33].

The region from 1450 to 1500 cm^{-1} is associated to $\nu_{(N–CS2)}$. The position of this band in IR spectra in general is found in between a single and a double C–N bond. The band at 1070–930 cm^{-1}, $\nu_{asy(C–S)}$, contributes to determining the coordination mode of the dithiocarbamate. In bidentate coordination, a single absorption is observed in this region. In the case of asymmetrical bonding, the $\nu_{asy(C–S)}$ is a split band. However, if the ligand is monodentate, the split band separates further [33].

For sodium salts, [Na{S_2CN(Me)R}], the $\nu_{(N–CS2)}$ and $\nu_{asy(C–S)}$ values previously reported are 1474 and 966 cm^{-1} for R = $CH_2CH(OMe)_2$, and 1473 and 982 cm^{-1} for (R = 2-methyl-1,3-dioxolane) [32]. The $\nu_{(N–CS2)}$ were 1429–1501 cm^{-1} for **1–6**, indicating an increase in its double bond character when compared to the sodium salt. This also confirms the symmetric bidentate coordination, since only one band associated with the C–S asymmetric stretch was observed in the IR spectra.

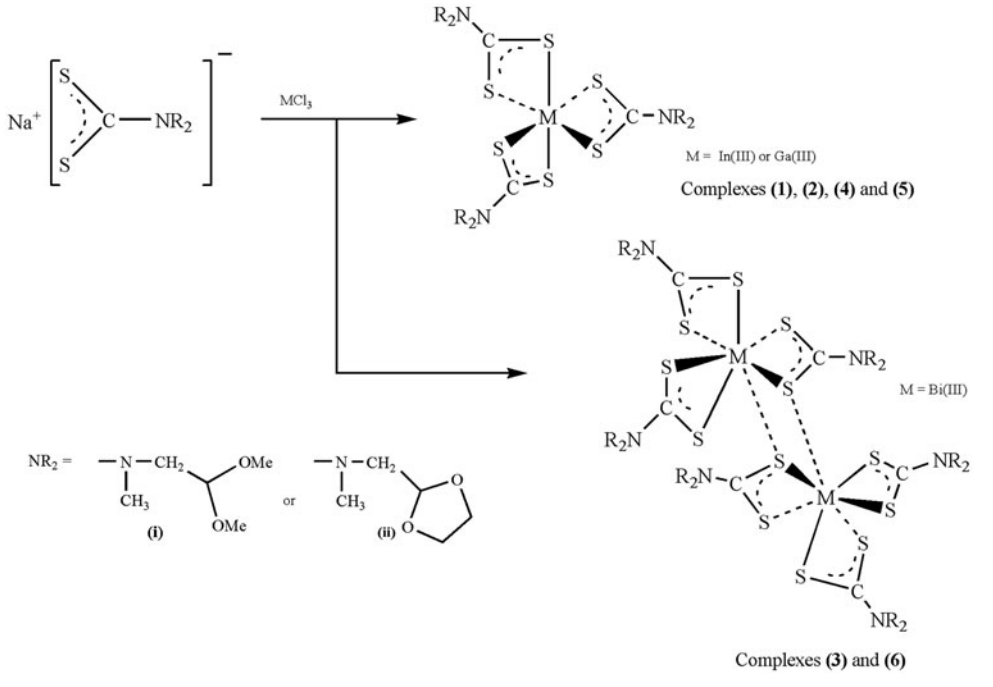

Scheme 1. Synthetic route for **1–6**.

There was little variation in the ^{1}H and ^{13}C NMR signals of the ligand upon coordination. A close relationship between ^{13}C chemical shift, δ and $\nu(N–CS_2)$ has been observed in this work. Higher values of the stretching frequency of N–C indicate a higher double bond character. It effects π-electron circulation at the N–C contact, and therefore decreases the net magnetic field experienced by the $N^{13}CS_2$, since it locates in the diamagnetic zone of the molecule [34]. Consequently, lower values of ^{13}C chemical shift (δ) have been observed.

$[In\{S_2CNR(R^1)\}_3]$ (**1**), $[Bi\{S_2CNR(R^1)\}_3]$ (**3**), and $[Bi\{S_2CNR(R^2)\}_3]$ (**6**) {R = Me; R^1 = $CH_2CH(OMe)_2$ and R^2 = 2-methyl-1,3-dioxolane} crystallize in the triclinic system with *P-1* and $Z = 2$ (table 1). $[In\{S_2CNR(R^2)\}_3]$ (**4**) crystallizes in the monoclinic system with $P2_1/n$ and $Z = 4$. C5 in **1** and C17 in **4** of the $–CH_2CH(OMe)_2$ group were found disordered.

In **1** and **4,** DTC is bidentate, forming three chelate rings, assembling a mill wheel with three blades (figures 1 and 2).

The In–S, bonds are a little asymmetric, varying from 2.5496(8) Å, In–S6, to 2.6224(9) Å, In–S3, in **1**, and in **4,** the shorter bond is 2.5795(7) Å, In–S4, and the longer In–S3 is at 2.6110(7) Å (table 2). The In–S, bonds in **1** are more asymmetric not only in comparison to **4** but also in view of some known In(III)–DTC derivatives in the literature, where the shorter In–S bond is 2.562(2) Å and the longer one 2.615(2) Å [35].

Analogous with other published In–DTC complexes, **1** and **4** display a distorted octahedral geometry with different S–In–S angles, S5–In1–S3 = 151.98(3)°, S4–In1–S1 = 152.23 (3)°, and S6–In1–S2 = 163.74(3)° in **1**, and S6–In1–S3 = 151.02(2)°, S4–In1–S1 = 156.68 (2)°, and S5–In1–S2 = 151.55(2) in **4**.

Table 1. Crystallographic parameters for **1–6**.

Compound	**1**	**3**	**4**	**6**
Empirical formula	$C_{18}H_{36}N_3O_6S_6In$	$C_{18}H_{36}N_3O_6S_6Bi$	$C_{18}H_{30}N_3O_6S_6In$	$C_{18}H_{30}N_3O_6S_6Bi$
Formula weight	697.68	791.84	691.63	785.79
Temperature, K	293 (2)	293 (2)	293 (2)	293 (2)
Wavelength, Å	0.71073; Kα Mo	0.71073; Kα Mo	0.71073; Kα Mo	0.71073; Kα Mo
Crystal system	Triclinic	Triclinic	Monoclinic	Triclinic
Space group	*P-1*	*P-1*	$P2_1/n$	*P-1*
Unit cell dimensions				
a, Å	6.5169 (2)	9.9371 (3)	13.0868 (4)	10.0970 (5)
b, Å	15.7901 (7)	10.8247 (4)	10.3485 (2)	12.0620 (6)
c, Å	16.6972 (8)	14.4890 (5)	21.0881 (5)	13.7475 (6)
α, °	64.174 (4)	92.701 (3)	90	64.660 (4)
β, °	88.742 (3)	99.627 (3)	101.875 (3)	69.561 (4)
γ, °	78.670 (3)	95.706 (3)	90	66.473 (4)
Volume, $Å^3$	1512.49 (11)	1525.73 (9)	2794.81 (12)	1354.90 (11)
Z	2	2	4	2
Density (Calcd), $Mg\,m^{-3}$	1.532	1.724	1.644	1.926
Absorption coefficient, mm^{-1}	1.230	6.223	1.331	7.007
F (0 0 0)	716	784	1408	772
Crystal size, mm	0.4305 × 0.3694 × 0.0683	0.3908 × 0.1363 × 0.1144	0.39 × 0.21 × 0.07	0.3236 × 0.1030 × 0.0355
θ Range for data coll., °	2.40–26.37	1.89–26.37	1.97–26.37	1.96–26.73
Index ranges	$-8 \le h \le 8$ $-19 \le k \le 19$ $-20 \le l \le 20$	$-12 \le h \le 12$ $-13 \le k \le 13$ $-18 \le l \le 18$	$-16 \le h \le 16$ $-12 \le k \le 12$ $-25 \le l \le 26$	$-12 \le h \le 8$ $-15 \le k \le 13$ $-17 \le l \le 13$
Reflections collected/unique	17316/6174 [*R*(int) = 0.0309]	24550/6255 [*R*(int) = 0.0359]	21462/5706 [*R*(int) = 0.0295]	9744/5734 [*R*(int) = 0.0432]
Data completeness to $\theta = 26.37$	100.0%	100.0%	100.0%	99.4%
Refinement method	Full-matrix least squares on F^2	Full-matrix least squares on F^2	Full-matrix least-squares on F^2	Full-matrix least squares on F^2
Data/restraints/parameters	6174/2/317	6255/2/317	5706/0/307	5556/0/310
Absorption correction	Analytical	Analytical	Analytical	Analytical
Goodness-of-fit on F^2	1.138	1.148	1.035	1.033
Final *R* indices [$I > 2\sigma(I)$]	*R1* = 0.0333, *wR2* = 0.0819	*R1* = 0.0207, *wR2* = 0.0461	*R1* = 0.0273, *wR2* = 0.0580	*R1* = 0.0343, *wR2* = 0.0698
R indices (all data)	*R1* = 0.0436, *wR2* = 0.0872	*R1* = 0.0263, *wR2* = 0.0599	*R1* = 0.0387, *wR2* = 0.0639	*R1* = 0.0445, *wR2* = 0.0741
CCDC Ref.	971738	971739	971740	971741

In **3** and **6,** dithiocarbamate binds bismuth via an anisobidentate coordination mode. The six sulfurs, which coordinate Bi(III), are a pentagonal pyramid, where the stereochemically active electron pair locates at the base of the pyramid. Among the five equatorial Bi–S bonds, three are long [2.9650(9) Å; Bi–S2, 2.8864(10) Å; Bi–S4, 2.7888(9) Å; Bi–S6 in **3** and 2.9110(12) Å; Bi–S2, 2.8719(13) Å; Bi–S4, 2.9303(12) Å; Bi–S6 in **6**] and the other two are short [2.8261(10) Å; Bi–S1, and 2.7693(9) Å; Bi–S4 in **3**, 2.7663(12) Å; Bi–S3 and 2.7924(13) Å; Bi–S5 in **6**]. Apical Bi–S bonds are much shorter than the others [2.6118(9) Å, Bi–S5 in **3** and 2.5668(14) Å, Bi–S1, in **6**] (figures 3 and 4).

The sum of the angles in the basal plane around Bi, S1–Bi–S2 61.69(3)°, S3–Bi–S6 77.22(3)°, S1–Bi–S2 61.69(3)°, S4–Bi–S3 64.48(3)°, S4–Bi–S1 79.90(3)° and S6–Bi–S2

Table 2. Selected bond lengths and angles for **1–6**.

[In{$S_2CNR(R^1)$}$_3$] (**1**)	In–S1	2.5983(9)	In–S6	2.5496 (8)	C13–S5	1.724 (3)
	In–S2	2.5823 (9)	C1–S1	1.717 (3)	C13–S6	1.722 (3)
	In–S3	2.6224 (9)	C1–S2	1.729 (3)	C1–N1	1.321 (4)
	In–S4	2.5953 (8)	C7–S3	1.713 (3)	C7–N2	1.334 (4)
	In–S5	2.6215 (9)	C7–S4	1.723 (3)	N3–C13	1.328 (4)
	S2–In1–S3	106.86 (3)	S5–In1–S3	151.98 (3)	S2–In1–S1	69.68 (3)
	S2–In1–S5	98.89 (3)	S4–In1–S1	152.23 (3)	S4–In1–S3	69.25 (3)
	S6–In1–S3	86.79 (3)	S6–In1–S2	163.74 (3)	S6–In1–S5	69.90 (3)
[Bi{$S_2CNR(R^1)$}$_3$] (**3**)	Bi–S1	2.8261 (10)	Bi–S2^i	3.2497 (10)	C13–S5	1.744 (4)
	Bi–S2	2.9650 (9)	C1–S1	1.725 (3)	C13–S6	1.697 (4)
	Bi–S3	2.7887 (9)	C1–S2	1.713 (4)	C1–N1	1.334 (4)
	Bi–S4	2.7693 (9)	C7–S3	1.713 (4)	C7–N2	1.330 (4)
	Bi–S5	2.6118 (9)	C7–S4	1.721 (4)	N3–C13	1.329 (4)
	Bi–S6	2.8864 (10)				
	S1–Bi–S2	61.69 (3)	S6–Bi–S2	76.62 (3)	S5–Bi–S4	87.92 (3)
	S3–Bi–S6	77.22 (3)	S5–Bi–S1	91.48 (3)	S5–Bi–S6	65.39 (3)
	S4–Bi–S3	64.48 (3)	S5–Bi–S2	87.42 (3)		
	S4–Bi–S1	79.90 (3)	S5–Bi–S3	86.42 (3)		
[In{$S_2CNR(R^2)$}$_3$] (**4**)	In–S1	2.5961 (7)	In–S6	2.5963 (7)	C13–S5	1.717 (3)
	In–S2	2.6109 (7)	C1–S1	1.719 (3)	C13–S6	1.724 (3)
	In–S3	2.6110 (7)	C1–S2	1.723 (2)	C1–N1	1.326 (3)
	In–S4	2.5795 (7)	C7–S3	1.712 (3)	C7–N2	1.328 (3)
	In–S5	2.5895 (8)	C7–S4	1.725 (2)	N3–C13	1.325 (3)
	S2–In1–S3		S6–In1–S3	151.02 (2)	S2–In1–S1	69.23 (2)
	S2–In1–S5		S4–In1–S1	156.68 (2)	S4–In1–S3	69.39 (2)
	S6–In1–S3		S5–In1–S2	151.55 (2)	S6–In1–S5	69.51 (2)
[Bi{$S_2CNR(R^2)$}$_3$] (**6**)	Bi–S1	2.5668 (14)	Bi–S6^i	3.3222 (14)	C13–S5	1.727 (5)
	Bi–S2	2.9110 (12)	C1–S1	1.745 (5)	C13–S6	1.716 (5)
	Bi–S3	2.7663 (12)	C1–S2	1.689 (6)	C1–N1	1.332 (6)
	Bi–S4	2.8719 (13)	C7–S3	1.718 (5)	C7–N2	1.329 (6)
	Bi–S5	2.7924 (13)	C7–S4	1.719 (5)	N3–C13	1.331 (6)
	Bi–S6	2.9303 (12)				
	S2–Bi–S6	77.05 (4)	S5–Bi–S6	62.28 (3)	S1–Bi–S5	90.88 (5)
	S3–Bi–S5	72.78 (4)	S1–Bi–S2	65.18 (4)	S1–Bi–S6	87.33 (4)
	S3–Bi–S4	63.34 (4)	S1–Bi–S3	79.91 (4)		
	S4–Bi–S2	88.09 (4)	S1–Bi–S4	93.34 (5)		

Symmetry codes: (i) $-x+1, -y+1, -z+1$ for **3** and (i) $-x+1, -y+1, -z$ for **6.**

76.62(3)° is 359.61° in **3**; S2–Bi–S6 77.05(4)°, S3–Bi–S5 72.78(4)°, S3–Bi–S4 63.34(4)°, S4–Bi–S2 88.09(4)° and S5–Bi–S6 62.28(4)° and 363.54° in **6**. These small deviations from the expected 360° support the proposal of distorted pentagonal pyramidal coordination.

A weak Bi–S intermolecular interaction is observed at 3.3222(14) Å (Bi–S6^i) in **3** and 3.2497(10) Å (Bi–S2^i) in **6**, in the direction of the lone pair forming a dimeric structural arrangement. These distances are shorter than the sums of the corresponding van der Waals radii, 4.2 Å [36]. In **3**, the Bi–S intermolecular interaction occurs between neighboring molecules, however in **6,** the molecules are not in the same unit cell (figure 1).

There are no significant intra and intermolecular hydrogen interactions involving the metal cation. Bi(III)-containing DTC complexes are normally six-coordinate with no Bi–S

intermolecular contact. However, similar distorted pentagonal pyramidal geometry and dimeric associations have been previously described for bismuth dithiocarbamate complexes [37–39].

The N–C bond lengths of DTC are between 1.321(4) and 1.338(4) Å, suggesting a partial double bond character, as a consequence of a higher electron density expected for the complexes, confirming the delocalization of electron density in the dithiocarbamate, as revealed by IR and ^{13}C NMR experiments. The C–S bond lengths range from 1.689(6) to 1.745(5) Å in **3** and 1.697(4)–1.744(4) Å in **6**. In **3** and **6,** one C–S bond is shorter than the other in agreement with asymmetric Bi–S bonds.

3.3. *Biocide activity of 1–6*

Aspergillosis deserves special attention due to the growing number of deaths from fungal infections in individuals who are immunocompromised either from the action of immunosuppressive drugs, diseases, cancer, or AIDS, or as the resulting resistance to drugs employed in *Aspergillosis* [40].

In this work, the biocide assays of $[In\{S_2CNR(R^1)\}_3]$ (**1**), $[Ga\{S_2CNR(R^1)\}_3]$ (**2**), $[Bi\{S_2CNR(R^1)\}_3]$ (**3**), $[In\{S_2CNR(R^2)\}_3]$ (**4**), $[Ga\{S_2CNR(R^2)\}_3]$ (**5**), and $[Bi\{S_2CNR(R^2)\}_3]$ (**6**) {R = Me; $R^1 = CH_2CH(OMe)_2$ and R^2 = 2-methyl-1,3-dioxolane} were performed in terms of inhibitory concentrations. Pre-screening against *A. niger*, *A. parasiticus*, and *P. citrinum* have been performed with **1–6** at a concentration of 250 μg mL^{-1}, according to a pre-established protocol [41]. Experiments of IC_{90} and IC_{50} were only performed for those complexes with 100% inhibition growth of the studied micro-organism in this concentration of 250 μg mL^{-1}.

None of the complexes displayed better efficiency than miconazole nitrate, which showed a wide range of biocide action, however little selectivity against all fungi (table 3). Our complexes were quite selective in the presence of the micro-organisms.

Concerning biocide activity against *A. niger*, we observe lower IC_{90} of **1**, **3**, **4,** and **6**, 44.8, 19.7, 22.6, and 39.8 μM L^{-1}, than nystatin, 67.5 μM L^{-1}, with **3** the more active. However, the In(III) complexes, **1** and **4**, were more efficient than the other DTC and the control drug, in terms of IC_{50} concentration, 0.699 and 2.82 μM L^{-1}. The Bi(III) derivatives, **3** and **6**, were quite efficient to reduce the population of *A. parasiticus*. The IC_{90}, 39.5 and 79.5 μM L^{-1}, and IC_{50}, 0.308 and 9.94 μM L^{-1}, were much lower than values obtained for

Table 3. Inhibition concentration of 90% (IC_{90}) and 50% (IC_{50}) (μM L^{-1}) for **1–6**.

	A. niger		*A. parasiticus*		*P. citrinum*	
Complexes	IC_{90}	IC_{50}	IC_{90}	IC_{50}	IC_{90}	IC_{50}
$[In\{S_2CNR(R^1)\}_3]$ (**1**)	44.8	0.699	179.2	89.6	179.2	5.59
$[Ga\{S_2CNR(R^1)\}_3]$ (**2**)	191.5	23.94	383.1	191.5	191.5	95.77
$[Bi\{S_2CNR(R^1)\}_3]$ (**3**)	19.7	9.87	39.5	0.308	157.9	4.93
$[In\{S_2CNR(R^2)\}_3]$ (**4**)	22.6	2.82	361.5	90.4	180.7	1.41
$[Ga\{S_2CNR(R^2)\}_3]$ (**5**)	193.3	24.17	386.7	193.3	386.7	96.66
$[Bi\{S_2CNR(R^2)\}_3]$ (**6**)	39.8	19.88	79.5	9.94	39.77	19.88
$Na[S_2CNR(R^1)]$ **(i)**	575.4	143.86	1150.9	575.4	575.4	287.7
$Na[S_2CNR(R^2)]$ **(ii)**	5811.7	2905.8	11623.4	5811.7	11623.4	2905.8
Nystatin	67.5	16.87	269.9	67.5	>269.9	269.9
Miconazole nitrate	2.04	0.446	1.02	0.000124	65.23	32.61

Note: R = Me; R^1 = CH2CH(OMe)2 and R^2 = 2-methyl-1,3-dioxolane.

nystatin and the other complexes. All complexes, except **5**, displayed remarkable activity against *P. citrinum*, much lower than nystatin. Bi(III) complexes **3** and **6** were more efficient to reduce 90% of the fungus population, 157.9 and 39.77 μM L^{-1}, respectively. However, within the incubation time of 48 h, **4** displayed smaller IC_{50}, 1.41 μM L^{-1}, followed by **3**, 4.93 μM L^{-1}, **1**, 5.59 μM L^{-1}, and **6**, 19.88 μM L^{-1}. All complexes were more active than nystatin, IC_{50} = 269.9 μM L^{-1}. This preliminary testing led us to conclude that **3** and **6** displayed the best antifungal activities, followed by **4**. The close relationship between structure and biological activity is well established. It is not surprising that Bi(III) derivatives exhibit better biocide activity than the Ga(III) and In(III) ones. Bi(III)-based complexes are remarkable, as pointed out in recent publications [42]. Since the chemical environment at Bi(III) in **3** and **6** are roughly the same, the better efficiency of the former derivative in comparison to the latter might relate to the nature of the R group that comprises the DTC. Because of the aliphatic chain, the degree of freedom of the $CH_2CH(OMe)_2$ fragment in **3** is higher than that of 2-methyl-1,3-dioxolane, a cyclic group, in **6**. The –OMe can freely rotate along the –CH–O– bond allowing perfect conformations for long distance CH–O–H interaction with specific sites of vital molecules in the micro-organism. Such interactions might deactivate important biological processes for cell survival. The cyclic group, more rigid, in **6** might frustrate such interactions, diminishing its biocide activity.

4. Conclusion

Most literature concerning main group metal-based DTC concerns the biocide activity of organotin derivatives [43, 44]. Little has been done for Ga(III), In(III), and Bi(III) coordinated to DTCs. The synthesis, characterization, and biological aspects of new [M{$S_2CNR(R^1)$}$_3$] complexes {M = Ga(III), In(III) and Bi(III), R = Me; $R^1 = CH_2CH(OMe)_2$ and R^2 = 2-methyl-1,3-dioxolane} have been the focus of this report. Three species of fungi have been cultivated in the presence of **1–6**. Despite the poor activity compared to miconazole nitrate, all complexes display selectivity towards the micro-organims and an interesting activity in comparison to the nystatin, a well-known remedy for clinical use. Complexes **3** and **6** were more active in terms of the IC_{90} and IC_{50} results followed by **4**. Due to the growing fatal cases of *Aspergillosis*, the investigation of potential drugs is quite important. In addition, in view of the number of Bi(III)-derivatives in clinical use, we believe **3** and **6** might become candidates for more advanced testing, since Bi(III) drugs are safe and effective in the treatment of a variety of microbial infections, and display low toxicity for patients and for the environment.

Supplementary material

Crystallographic data are available on request at Cambridge Crystallographic Data Center on quoting the deposition numbers CCDC 971738 (**1**), 971739 (**3**), 971740 (**4**), and 971741 (**6**).

Acknowledgement

This work was supported by CNPq and FAPEMIG – Brazil.

References

[1] E.R.T. Tiekink, D.J. Young. *J. Chem. Crystallogr.*, **38**, 419 (2008).
[2] H.D. Yin, J. Zhai, Y.Y. Sun, D.Q. Wang. *Polyhedron*, **27**, 663 (2008).
[3] E.R.T. Tiekink. *Appl. Organomet. Chem.*, **22**, 533 (2008).
[4] F.W. Sunderman. *Ann. Clin. Lab. Sci.*, **9**, 1 (1979).
[5] D.L. Bodenner, P.C. Dedon, P.C. Keng, R.F. Borch. *Cancer Res.*, **46**, 2745 (1986).
[6] J.J. Suh, H.M. Pettinati, K.M. Kampman, C.P. O'Brien. *J. Clin. Psychopharm.*, **26**, 290 (2006).
[7] B. Cvek, Z. Dvorak. *Curr. Pharm. Des.*, **13**, 3155 (2007).
[8] P.J. Nieuwenhuizen, J. Reedijk, M. Van Duin, W.J. McGill. *Rubber Chem. Technol.*, **70**, 368 (1997).
[9] M. Cicotti. Compound class: alkylenebis(dithiocarbamates). In *Handbook of Residue Analytical Methods for Agrochemical*, P.W. Lee, H. Aizawa, A.C. Barefoot, J.J. Murphy (Eds.), Vol. 2, pp. 1089–1098, Wiley, Chichester (2003).
[10] D. Fan, M. Afzaal, M.A. Mallik, C.Q. Nguyen, P. O'Brien, P.J. Thomas. *Coord. Chem. Rev.*, **251**, 1878 (2007).
[11] N. Yang, H. Sun. *Coord. Chem. Rev.*, **251**, 2354 (2007).
[12] H. Li, C.S. Lai, J. Wu, P.C. Ho, D. de Vos, E.R.T. Tiekink. *J. Inorg. Biochem.*, **101**, 809 (2007).
[13] H.P.S. Chauhan, B. Abhilasha, B. Sumit. *Appl. Organomet. Chem.*, **24**, 317 (2010).
[14] M.J. Clarke, F. Zhu, D.R. Frasca. *Chem. Rev.*, **99**, 2511 (1999).
[15] M. Thiel, T. Schilling, D.C. Gey, R. Ziegler, P. Collery, B.K. Keppler. *Contr. Oncol.*, **54**, 439 (1999).
[16] L.R. Bernstein, T. Tanner, C. Godfrey, B. Noll. *Met. -Based Drugs*, **7**, 33 (2000).
[17] J.G. da Silva, C.C.H. Perdigão, N.L. Speziali, H. Beraldo. *J. Coord. Chem.*, **66**, 385 (2013).
[18] J.A. Lessa, M.A. Soares, R.G. dos Santos, I.C. Mendes, L.B. Salum, H.N. Daghestani, A.D. Andricopulo, B.W. Day, A. Vogt, H. Beraldo. *Biometals*, **26**, 151 (2013).
[19] J.P. André, H.R. Mäcke. *J. Inorg. Biochem.*, **97**, 315 (2003).
[20] D.C. Menezes, F.T. Vieira, G.M. de Lima, A.O. Porto, M.E. Cortés, J.D. Ardisson, T.E. Albrecht-Schmitt. *Eur. J. Med. Chem.*, **40**, 1277 (2005).
[21] R.A. Howie, G.M. de Lima, D.C. Menezes, J.L. Wardell, S.M.S.V. Wardell, D.J. Young, E.R.T. Tiekink. *Cryst. Eng. Comm.*, **10**, 1626 (2008).
[22] D.C. Menezes, G.M. de Lima, A.O. Porto, C.L. Donnici, J.D. Ardisson, A.C. Doriguetto, J. Ellena. *Polyhedron*, **23**, 2103 (2004).
[23] D.C. Menezes, G.M. de Lima, A.O. Porto, F.A. Carvalho, M.G. Coelho, R. Augusti, J.D. Ardisson. *Appl. Organomet. Chem.*, **24**, 650 (2010).
[24] D.C. Menezes, F.T. Vieira, G.M. de Lima, J.L. Wardell, M.E. Cortés, M.P. Ferreira, M.A. Soares, A.V. Vilas Boas. *Appl. Organomet. Chem.*, **22**, 221 (2008).
[25] D.C. Menezes, G.M. de Lima, C.A. Cavalcanti, J.A.F. dos Santos, I.P. Ferreira, E.B. Paniago, J.L. Wardell, S.M.S.V. Wardell, K. Krambrock, I.C. Mendes, H. Beraldo. *J. Mol. Struct.*, **988**, 1 (2011).
[26] I.P. Ferreira, G.M. de Lima, E.B. Paniago, J.A. Takahashi, K. Krambrock, C.B. Pinheiro, J.L. Wardell, L.C. Visentin. *J. Mol. Struct.*, **1048**, 357 (2013).
[27] G.M. Sheldrick. *Acta Crystallogr., Part A*, **64**, 112 (2008).
[28] G.M. Sheldrick. *SHELXL-97, Program for Crystal Structure Refinement*, University of Göttingen, Germany (1997).
[29] C.K.C.C. Johnson, In *Crystallographic Computing*, F.R. Ahmed (Ed.), pp. 207–219, Munksgaard, Copenhagen, (1970).
[30] L.J. Farrugia. *J. Appl. Crystallogr.*, **30**, 565 (1997).
[31] C.F. Macrae, P.R. Edgington, P. McCabe, E. Pidcock, G.P. Shields. *J. Appl. Crystallogr.*, **39**, 453 (2006).
[32] I.P. Ferreira, G.M. de Lima, E.B. Paniago, W.R. Rocha, J.A. Takahashi, C.B. Pinheiro, J.D. Ardisson. *Eur. J. Med. Chem.*, **58**, 493 (2012).
[33] D.A. Brown, W.K. Glass, M.A. Burke. *Spectrochim. Acta, Part A*, **32**, 137 (1976).
[34] H.L.M. Vangaal, J.W. Diesveld, F.W. Pijpers, J.G.M. Vanderlinden. *Inorg. Chem.*, **18**, 3251 (1979).
[35] J.H. Park, M. Afzaal, M. Kemmler, P. O'Brien, D.J. Otway, J. Raftery, J. Waters. *J. Mater. Chem.*, **13**, 1942 (2003).
[36] C. Silvestru, H.J. Breunig, H. Althaus. *Chem. Rev.*, **99**, 3277 (1999).
[37] H.D. Yin, C.H. Wang, Y. Wang. *Appl. Organomet. Chem.*, **18**, 199 (2004).
[38] R.Z. Sun, Y.C. Guo, W.M. Liu, S.Y. Chen, Y.Q. Feng. *Chin. J. Struct. Chem.*, **31**, 655 (2012).
[39] H. Yin, F. Li, D. Wang. *J. Coord. Chem.*, **60**, 1133 (2007).
[40] C. Garcia-Vidal, D. Viasus, J. Carratalà. *Curr. Opin. Infect. Dis.*, **26**, 270 (2013).
[41] A.S. Zacchino, M.P. Gupta. *Manual de técnicas in vitro para la detección de compuestos antifúngicos*, pp. 85–99, Corpus Editorial y Distribuidora, Rosario (2007). (Spanish).
[42] J.A.R. Salvador, S.A.C. Fiqueiredo, R.M.A. Pinto, S.M. Silvestre. *Future Med. Chem.*, **4**, 1495 (2012).
[43] S.M. Abbas, S. Ali, S.T. Hussain, S. Shahzadi. *J. Coord. Chem.*, **66**, 2217 (2013).
[44] S. Jabbar, I. Shahzadi, R. Rehman, H. Iqbal, Q.U. Ain, A. Jamil, R. Kousar, S. Ali, S. Shahzadi, M.A. Choudhary, M. Shahid, Q.M. Khan, S.K. Sharma, K. Qanungo. *J. Coord. Chem.*, **65**, 572 (2012).